Langmuir

Article

pubs.acs.org/Langmuir

Bridging Adhesion of Mussel-Inspired Peptides: Role of Charge, Chain Length, and Surface Type

Wei Wei,[†] Jing Yu,[‡] Matthew A. Gebbie,[§] Yerpeng Tan,[∥] Nadine R. Martinez Rodriguez,[⊥] Jacob N. Israelachvili,[†,‡,§] and J. Herbert Waite*[,†,∥,⊥]

[†]Materials Research Lab, [‡]Department of Chemical Engineering, [§]Materials Department, [∥]Biomolecular Science and Engineering Program, and [⊥]Department of Molecular, Cell & Development Biology, University of California, Santa Barbara, Santa Barbara, California 93106, United States

Supporting Information

ABSTRACT: The 3,4-dihydroxyphenylalanine (Dopa)-containing proteins of marine mussels provide attractive design paradigms for engineering synthetic polymers that can serve as high performance wet adhesives and coatings. Although the role of Dopa in promoting adhesion between mussels and various substrates has been carefully studied, the context by which Dopa mediates a bridging or nonbridging macromolecular adhesion to surfaces is not understood. The distinction is an important one both for a mechanistic appreciation of bioadhesion and for an intelligent translation of bioadhesive concepts to engineered systems. On the basis of mussel foot protein-5 (Mfp-5; length 75 res), we designed three short, simplified peptides (15−17 res) and one relatively long peptide (30 res) into which Dopa was enzymatically incorporated. Peptide adhesion was tested using a surface forces apparatus. Our results show that the short peptides are capable of weak bridging adhesion between two mica surfaces, but this adhesion contrasts with that of full length Mfp-5, in that (1) while still dependent on Dopa, electrostatic contributions are much more prominent, and (2) whereas Dopa surface density remains similar in both, peptide adhesion is an order of magnitude weaker (adhesion energy $E_{ad} \sim -0.5$ mJ/m^2) than full length Mfp-5 adhesion. Between two mica surfaces, the magnitude of bridging adhesion was approximately doubled ($E_{ad} \sim -1$ mJ/m^2) upon doubling the peptide length. Notably, the short peptides mediate much stronger adhesion ($E_{ad} \sim -3.0$ mJ/m^2) between mica and gold surfaces, indicating that a long chain length is less important when different interactions are involved on each of the two surfaces.

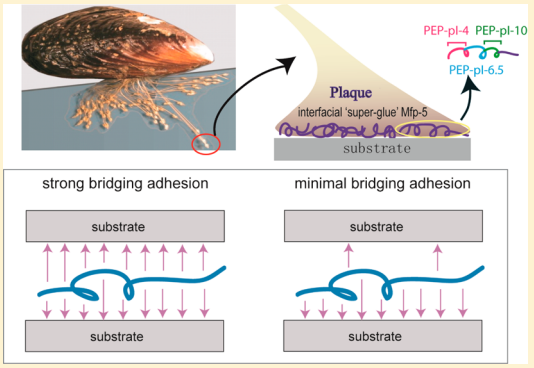

INTRODUCTION

Marine mussels and sandcastle worms use a suite of proteins rich in 3,4-dihydroxyphenyl-L-alanine (Dopa) to attach to diverse hard surfaces in the sea.[1,2] In 2006, an elegant demonstration of a strong (∼1 nN) but reversible interaction between a single tethered Dopa and a wet TiO_2 surface raised the possibility that any polymer backbone functionalized with Dopa might be rendered adhesive.[3,4] For a variety of reasons, this promise has remained elusive.[5−9] For example, a synthetic acrylamide copolymer functionalized with Dopamine achieved less than 70 pN of adhesion per catechol on TiO_2,[10] and most poly(ethylene glycol) constructs with Dopa show adhesion to biological surfaces only following oxidation with periodate.[11−14] To better understand the interplay between the surface activity of Dopa and its associated macromolecular backbone, Lin et al.[6] examined the adhesion to mica of two mussel foot proteins (mfp) with similar Dopa contents using a surface forces apparatus and identified two distinctly different Dopa-mediated adhesive modes, that is, a bridging and a nonbridging adhesive mode (Figure 1). In the first mode, molecules span the gap between two solid surfaces with adhesive interactions on both sides; in the second, molecules confine most of their adhesive interactions to one surface. One protein, mfp-3F, exhibited strong and rapid bridging adhesion between the mica surfaces, whereas the other, mfp-1, bound to one mica surface only with little to no tendency

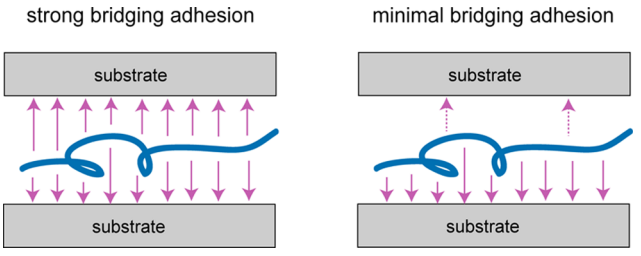

Figure 1. Cartoon of a molecule interacting with substrates in strong and minimal bridging adhesive modes. In the first mode, molecules span the gap between two solid surfaces with energetic interactions on both sides; in the second, molecules confine most of their energetic interactions to one surface.

Received: November 6, 2014
Revised: December 22, 2014
Published: December 24, 2014

DOI: 10.1021/la504316q
Langmuir 2015, 31, 1105−1112

to bridge over to the other side, except under high shear. Only two mussel foot proteins, mfp-3 and mfp-5, exhibit strong bridging adhesion. Not surprisingly, these proteins are localized to the interface between the plaque and the substratum. Of the mussel foot proteins, mfp-5 has the highest Dopa content (~30 mol %) and achieves an adhesion energy per unit area on mica that approaches the interaction between tethered biotin and avidin.[5] On the basis of the known primary sequence of mfp-5, we explore the following questions here: (1) Do the amino acid sequences flanking Dopa affect bridging adhesion? (2) Do interactions besides those involving Dopa help to mediate the bridging adhesion of mfps?[15] (3) Is bridging adhesion dependent on chain length and surface type?

To address these questions, three mfp-5-inspired peptides 15−16 residues long were prepared with and without enzymatic modification of tyrosine (Y → Y* denotes Tyr to Dopa): VGSGY*DGY*SDGY*Y*DG (PEP-pI-4), HY*HSGGSY*-HGSGY*HG (PEP-pI-6.5), GY*KGKY*Y*GKG KKY*YY*K (PEP-pI-10) (Figure 2 and Figure S1). The effect of chain length on bridging adhesion was tested by also preparing a peptide consisting of the PEP-pI-4 sequence repeated twice in a linear fashion (PEP-pI-4-dimer). Our rationale in selecting these particular peptides was that they represent more than half the sequence and most of the sequence diversity of mfp-5 with the smallest possible number of amino acids. The repulsive and attractive forces of these peptides on mica and gold surfaces were investigated with a surface forces apparatus (SFA).[16]

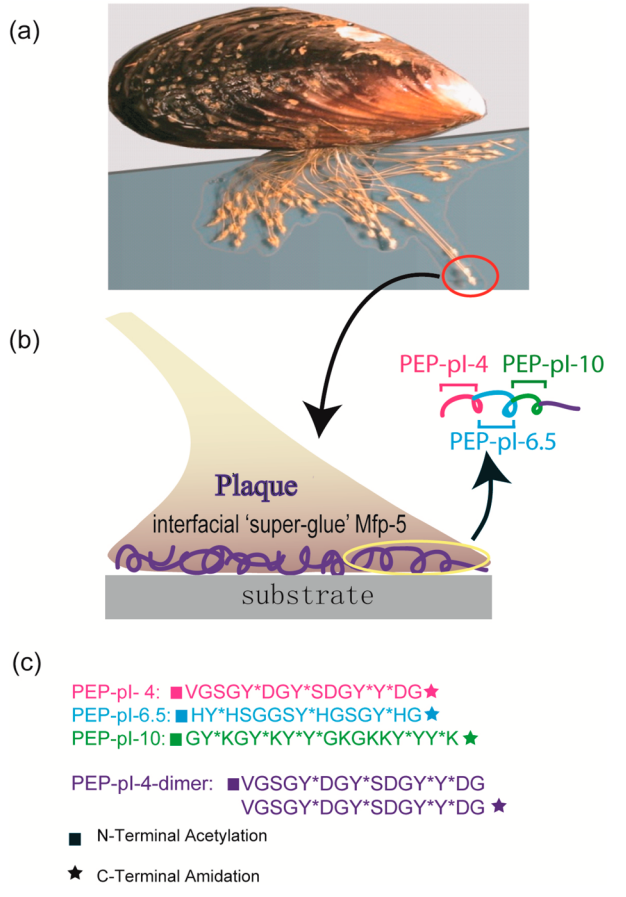

Figure 2. Dissecting mussel adhesive protein mfp-5 into distinct peptides. (a) An adult mussel attached to a glass surface by a byssus containing many threads and adhesive plaques. (b) Schematic zoom of a plaque, showing the "super glue" mfp-5 at the plaque interface. (c) Three unique sequences with 15−16 amino acid residues and representing about three-fifths of mfp-5 were selected from the parent sequence. All three short peptides have different pIs. A longer dimeric peptide was created by connecting two PEP-pI-4 monomers in tandem.

RESULTS

Peptide Modification. Mushroom tyrosinase is known to *o*-hydroxylate peptidyl Tyr to Dopa (Figure 3b) and was thus used for this purpose in the peptides.[17,18] The conversion by tyrosinase requires safeguards to minimize the formation of undesirable side products such as 3,4,5-trihydroxyphenylalanine (Topa) and Dopaquinone (Figure 3b).[17] By reversibly capturing Dopa immediately after it has formed, borate significantly improves Dopa yield and decreases side-reactions. After stopping the reaction, modified peptides were separated by reverse phase HPLC, which typically eluted three types of modified peptides, i.e., those that were (a) partially modified (some unmodified Tyr residues remain), (b) completely modified (every Tyr residue is modified), or (c) hypermodified (one or more Tyr residues were converted to Topa) peptides. Electrospray ionization mass spectrometry (ESI) and matrix assisted laser desorption ionization (MALDI) with time-of-flight (TOF) were used to measure the peptide masses in the eluting fractions (Figure S2). Those fractions with masses matching the calculated mass of completely modified (type b) peptides were pooled for amino acid analysis and sequencing by tandem MS. Amino acid analysis results demonstrate that the compositions of pure modified PEP-pI-4, PEP-pI-6.5, and PEP-pI-4-dimer are consistent with calculated masses: only traces of Tyr remained, and no Topa was detectable. For PEP-pI-10, there is one Tyr that persistently eludes conversion to Dopa: this is Y-14, the central member in the Y-triad. Contact between tyrosinase and Y-14 is presumably impeded by the bulky borate groups on Y*-13 and Y*-15 during the modification.

Bridging Adhesion of Short Peptides between Two Mica Surfaces. Bridging adhesion was measured in the surface forces apparatus (SFA) using an asymmetric configuration; that is, a monolayer of peptides (diameter of hydration ~2−3 nm) was adsorbed to one mica surface which was then brought into contact with the clean surface, compressed, and separated. Modified peptides PEP-pI-4, PEP-pI-6.5, and PEP-pI-10 all adhered to mica surfaces, with the strongest adhesion force, −4 mN/m (corresponding to a work of adhesion of 0.64 mJ/m^2), associated with PEP-pI-10. PEP-pI-6.5, although having the lowest Dopa content (only 3 Dopa out of 15 residues), exhibited an intermediate adhesion force of −3.0 mN/m, and the weakest adhesion force (−2.6 mJ/m) was observed for PEP-pI-4 (Figure 4a). These work of adhesion values are notable in being more than an order of magnitude less than full-length mfp-5, even though each peptide represents approximately a fifth of the native sequence. The most likely explanation for this vastly decreased adhesion relative to the native sequence is that the shortened 15−17 residue peptide chains have a much smaller probability of adsorbing in configurations where "loops" or "tails" of the peptides adsorbed onto one mica surface are of sufficient length to make a bridging contact with the opposing mica surface. As a result, most of the short peptides end up interacting intimately with one mica surface, and with few remaining groups available for intimate contact with the other surface, they rely on longer range Coulombic attractions, e.g., positive Lys or His to negative siloxyl groups, for adhesive bridging (Figure 1).

Consistent with previous work, the results confirm that Dopa plays an essential role in the adhesion of each of the peptides to

DOI: 10.1021/la504316q
Langmuir 2015, 31, 1105−1112

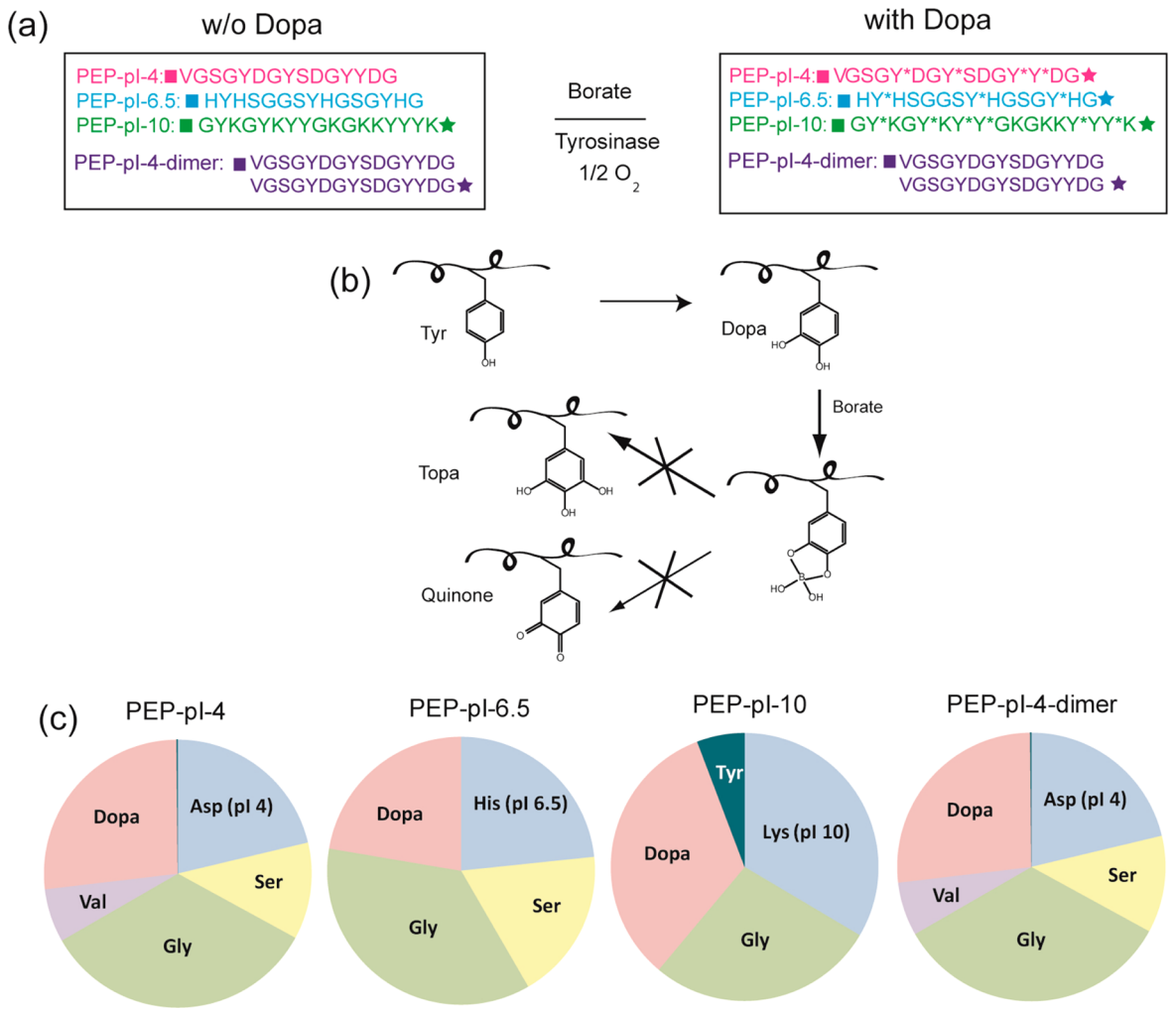

Figure 3. Preparation of synthetic mfp-5 inspired Dopa-containing peptides. (a) Tyr residues in the three different peptides were enzymatically hydroxylated to Dopa. However, (b) mushroom tyrosinase action is not limited to *o*-hydroxylation of Tyr but further converts Dopa to Dopa quinone or Topa. To avoid these reaction products, borate was added to capture Dopa by formation of a reversible borate–Dopa chelate complex. (c) Pie chart of amino acid composition of each modified peptide after enzymatic conversion and purification.

mica surfaces. All three peptides adhered most strongly to mica surfaces at pH 3 where Dopa is stable, and increasing the solution pH to 7.5, where much of the Dopa is quickly oxidized to the nonadhesive quinone form (Figure 3b), significantly reduced the measured adhesion: the work of adhesion dropped by 80%, 60%, and 35% for PEP-pI-6.5, PEP-pI-4, and PEP-pI-10, respectively, at pH 7.5 (Figure 4b). Previous tests on mussel proteins[5,9] have shown that Dopa undergoes auto-oxidation at pH 7.5, leading to diminished mfp adhesion. Given their derivation from mfp-5 sequences, the Dopa-containing peptides should be prone to similar oxidation tendencies. Notably, adhesion between two mica surfaces is never eliminated under Dopa oxidizing conditions, even for PEP-pI-4 at pH 7.5, where both the peptide and the mica surface are negatively charged. In addition to this residual adhesion, Dopa oxidation alone also fails to provide an explanation for why the pH affects the three short peptides so differently.

In addition to issues associated with Dopa auto-oxidation at alkaline pH, changes in peptide adhesion also reflect changing electrostatic interactions due to the protonation and/or deprotonation of amino acids and surface siloxyl groups.[19] Increasing pH significantly changes the charge densities (or the overall charge) in the three short peptides. At pH 3, PEP-pI-6.5 and PEP-pI-10 are both positively charged due to the histidine and lysine residues, respectively, so both can favorably interact with the negatively charged mica surface through attractive electrostatic interactions.[20] Increasing the solution pH to 7.5 greatly reduces the positive charges in PEP-pI-6.5; therefore, PEP-pI-6.5 loses both the hydrogen-bonding ability of Dopa to mica surfaces (due to oxidation) and the attractive electrostatic interactions offered by positive amino acid residues (by histidine deprotonation), which results in the largest decrease in terms of the percentage of the adhesion force (75% decrease). In comparison, the sign and density of the charges in PEP-pI-10 remain unchanged at pH 7.5, which enables PEP-pI-10 to maintain attractive interactions between two mica surfaces, despite depletion of Dopa by oxidation (35% decrease of adhesion).

Notably, PEP-pI-4 maintains high bridging adhesion between mica surfaces upon increasing the pH from 3 to 7.5, which would not be expected with both Dopa oxidation and carboxylate formation in PEP-pI-4, resulting in electrostatic repulsion between PEP-pI-4 and mica. The magnitude of the PEP-pI-4 adhesion only fell by 60%. One plausible explanation for this apparent anomaly is that interfacial proton concentration is rarely the same as that of the bulk[21] and that a strongly acidic

DOI: 10.1021/la504316q
Langmuir 2015, 31, 1105−1112

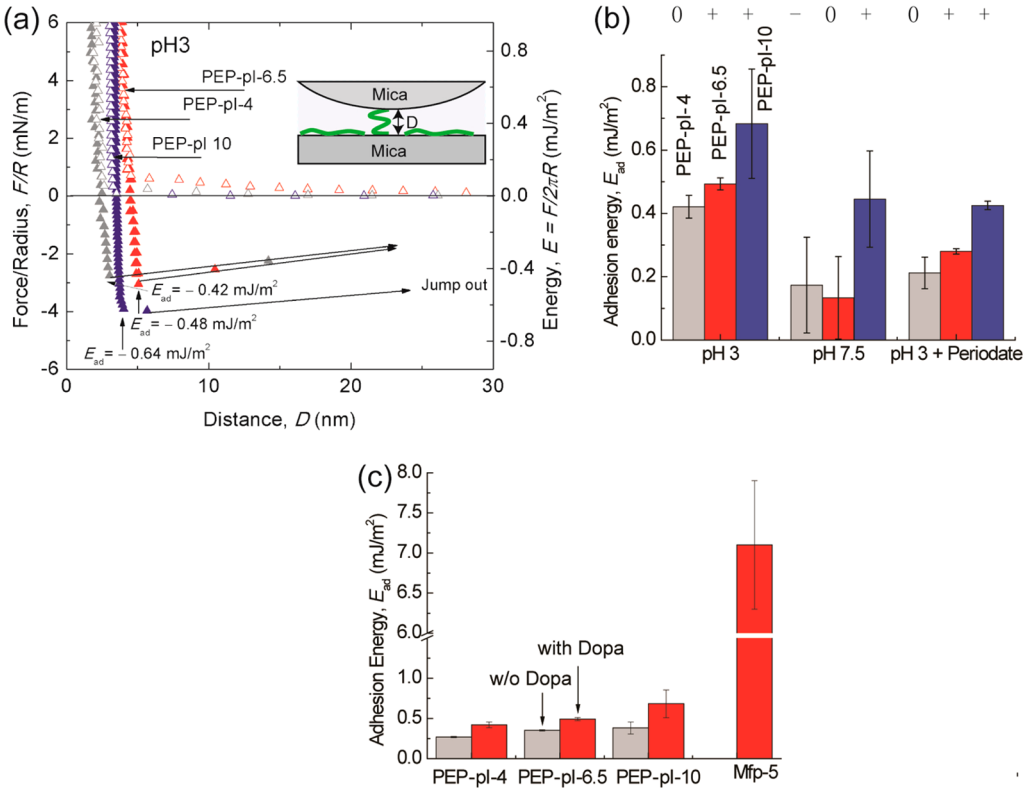

Figure 4. Adhesion to mica by mfp-5-derived peptides with and without Dopa. (a) Force−distance profiles of three short peptides in asymmetric configuration on mica surfaces. (b) Summary of adhesion energy of three short peptides measured in pH 3, pH 7.5, and pH 3 following periodate oxidation. '0", "+", and "−" represent respectively the neutral, positive, and negative charge the peptides carry at each condition. (c) Comparison of the adhesion energy of three short peptides with and without tyrosinase modification and mfp-5. The adhesion energies of three short peptides shown in (b) and (c) are averaged from between 6 and 12 repetitive force runs from two different experiments at each treatment. Mfp-5 data are from ref 8.

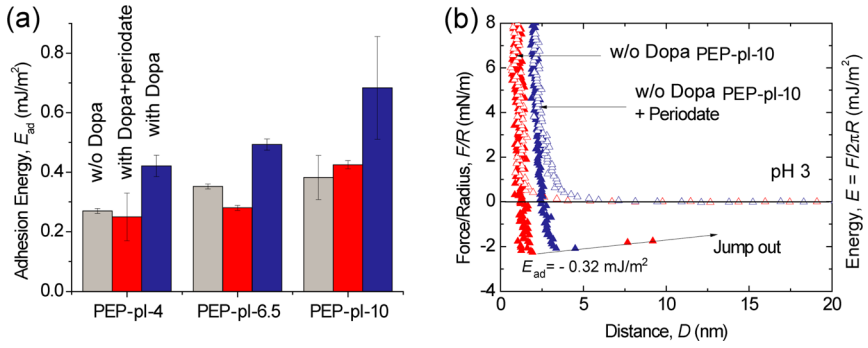

Figure 5. Effect of periodate oxidation on peptide adhesion. (a) Adhesion of three short peptides after periodate oxidation resembles the adhesion energy of three unmodified peptides. The adhesion energies are averaged from the values of 6−12 repeating force runs under each condition. (b) Force−distance curves of PEP-pI-10 before and after adding periodate but keeping the pH unchanged (pH = 3). Adding periodate did not change the adhesion force of unmodified PEP-pI-10, but the hard wall increased slightly.

interface such as that formed between mica and PEP-pI-4 can shield interfacial Dopa from the oxidation expected in solution at pH 7.5. Thus, the bidendate binding of intact Dopa would counteract the repulsion by the acidic groups.

The contribution of electrostatic interactions relative to H-bonding was explored by injecting periodate, an artificial oxidant, into the solution between two mica surfaces at pH 3: after periodate injection, all three peptides exhibited reductions in the measured attractive forces. Further, PEP-pI-6.5 and PEP-pI-4 exhibited higher adhesions at pH 3 with periodate than were measured at pH 7.5. The work of adhesion measured for PEP-pI-6.5 at pH 3 in the absence of Dopa residues is 0.28 mJ/m^2, almost 3 times the value measured at pH 7.5 (0.1 mJ/m^2). The work of adhesion for periodate-treated PEP-pI-4 was measured to be about twice as much as that at pH 7.5. Both of these observations implicate the involvement of electrostatic interactions in the binding of peptides to mica surfaces (Figure 4b).

To further resolve the relative contributions of charged residues and Dopa to the adhesion of three short peptides, SFA tests were performed on the unmodified peptides (without converting tyrosines to Dopa). The work of adhesion of the three unmodified peptides to mica surfaces ranged from 0.27 to 0.35 mJ/m^2 (Figure 4c), with trends similar to those seen with Dopa containing peptides, that is, PEP-pI-4 < PEP-pI-6.5 < PEP-pI-10, which come from electrostatic interactions as well as multiple Tyr-mediated monodentate H-bonds. Tyrosine conversion to

DOI: 10.1021/la504316q
Langmuir 2015, 31, 1105−1112

Dopa as much as doubled the adhesion energies on the same surface which further confirms the importance of Dopa for the bridging adhesion of all the peptides. After oxidizing the Dopa group in the peptides by periodate, the adhesion energies of three modified peptides dropped to values approaching the unmodified peptides, again indicating the effect of enzymatic modification (Figure 5a). No change of adhesion energy was observed for unmodified PEP-pI-10 (Figure 5b).

Bridging Adhesion of the PEP-PI-4-Dimer between Mica Surfaces. To evaluate how peptide length affects adhesion and to provide a better functional synthetic model system for bridging adhesion on mica, the PEP-pI-4-dimer sequence was subjected to evaluation by SFA. Increasing chain length should enhance the formation of loops and tails in the polymer chain. As π-cation interactions between aromatic and cationic residues in the peptides can complicate their conformation[22] as well as self-association,[23] the PEP-pI-4 sequence was chosen for the dimer study as the only peptide sequence without (pH-dependent) positively charged residues. The adhesive properties of this peptide dimer were characterized before and after mushroom tyrosinase modification by depositing the modified and unmodified peptide dimers onto a single freshly cleaved mica surface and then measuring the adhesive bridging of this peptide dimer to another mica surface. At pH 3, PEP-pI-4-dimer promotes adhesion between the mica surfaces of ~6 mN/m (corresponding to a work of adhesion of ~1 mJ/m^2) (Figure 6),

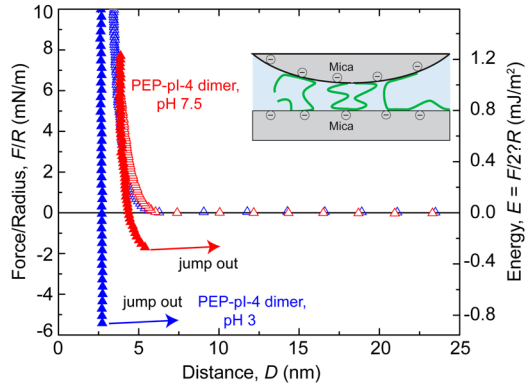

Figure 6. Force profiles of the Dopa-modified PEP-pI-4-dimer on mica at pH 3 and 7.5. Adhesion is approximately double that of the corresponding monomer in Figure 2 and shows similar losses due to auto-oxidation at pH 7.5.

which is approximately twice the adhesion exhibited by the PEP-pI-4 monomer sequence. Given that the pep-pI-4 monomer and dimer were deposited at the same solution mass fractions (as opposed to molar concentrations), surface Dopa amounts in two cases should be roughly equal. Higher adhesion of dimer should be due to its higher tendency of forming "loops" and "tails" which are favorable for bridging. As in the case of the short peptides, increasing pH to 7.5 decreased adhesion of PEP-pI-4-dimer to mica by approximately 65% to a value of about 0.35 mJ/m^2 due to Dopa oxidation. Since both the PEP-pI-4-dimer sequence and the mica surface should be negatively charged at this pH, the presence of residual adhesion is unexpected. Our explanation for this anomaly remains the same "interfacial pH" explanation that was invoked for the PEP-pI-4 monomer. The adhesion of unmodified PEP-pI-4-dimer (without Dopa) on mica at pH 3 was measured to be 0.4 mJ/m^2 (Figure S4), which is approximately half the adhesive energy measured for the Dopa-containing dimer. Interestingly, the adhesion measured for the unmodified PEP-pI-4-dimer was seen to be independent of pH for the pH 3 and 7.5 conditions tested in the current study (Figure S4). Tyrosine residues do not undergo autoxidation or deprotonation at pH 7.5 and may interact favorably with muscovite mica surfaces through either monodentate hydrogen bonds (analogous to the bidentate bonding exhibited by Dopa) or cation-π interactions with the K^+ ions that are present at mica surfaces.

Bridging Adhesion of PEP-PI-10 between Mica and Gold Surfaces. To test for bridging adhesion between dissimilar surfaces, SFA measurements were performed where one of the mica surfaces was replaced with a smooth gold surface (0.5 nm RMS roughness). PEP-pI-10 mediated the strongest adhesion between two mica surfaces (Figure 4a) and hence was selected for adhesive bridging between asymmetric mica/gold surfaces. PEP-pI-10 was first deposited onto mica where many of the Dopa groups form strong, specific interactions with the mica substrate, and this film was then compressed against an opposing gold surface at pH 3 (Figure 7). The adhesion of PEP-pI-10 in this

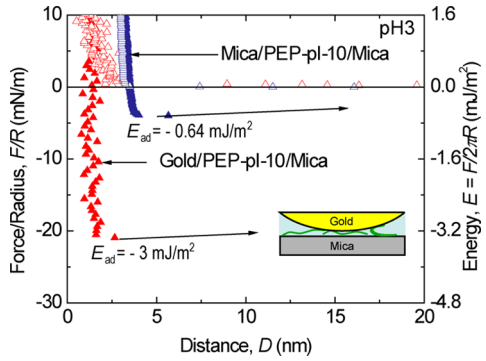

Figure 7. Force−distance profile of PEP-pI-10 coated on one mica surface against a gold surface. PEP-pI-10 showed 5 times stronger adhesion force in comparison to the adhesion force between two mica surfaces.

gold/peptide/mica geometry (~3 mJ/m^2) was much stronger than the adhesion measured in the mica/peptide/mica geometry. This strong adhesion is attributed to the high surface energy of gold, which has strong so-called "soft epitaxial" binding with Dopa, the other amino acid side chains, and backbone amides of protein/peptides.[24−28] As a result, PEP-pI-10 binds gold surfaces, even when most of the Dopa side chains have been recruited to the mica surface during the initial film deposition.

DISCUSSION

In previous SFA studies of mfp-based adhesion, little attention was given to the electrostatic interactions between mfps and substrates. In this work, however, the range of peptide ionizations enabled a systematic study of electrostatic contributions to adhesion in Dopa-containing systems. These measurements were performed at high salt concentration (0.35 M) that, like seawater, typically reduces the Debye length to ~0.5 nm. Here, we show that electrostatic interactions between mfps and substrates make a significant contribution to bridging adhesion. These results also highlight the importance of electrostatic interactions in highly concentrated electrolyte solutions, which are typically ignored. Electrostatic interactions are advantageous in that they are nonspecific and long-range in nature (potentially extending over several nanometers), whereas Dopa-mediated

DOI: 10.1021/la504316q
Langmuir 2015, 31, 1105−1112

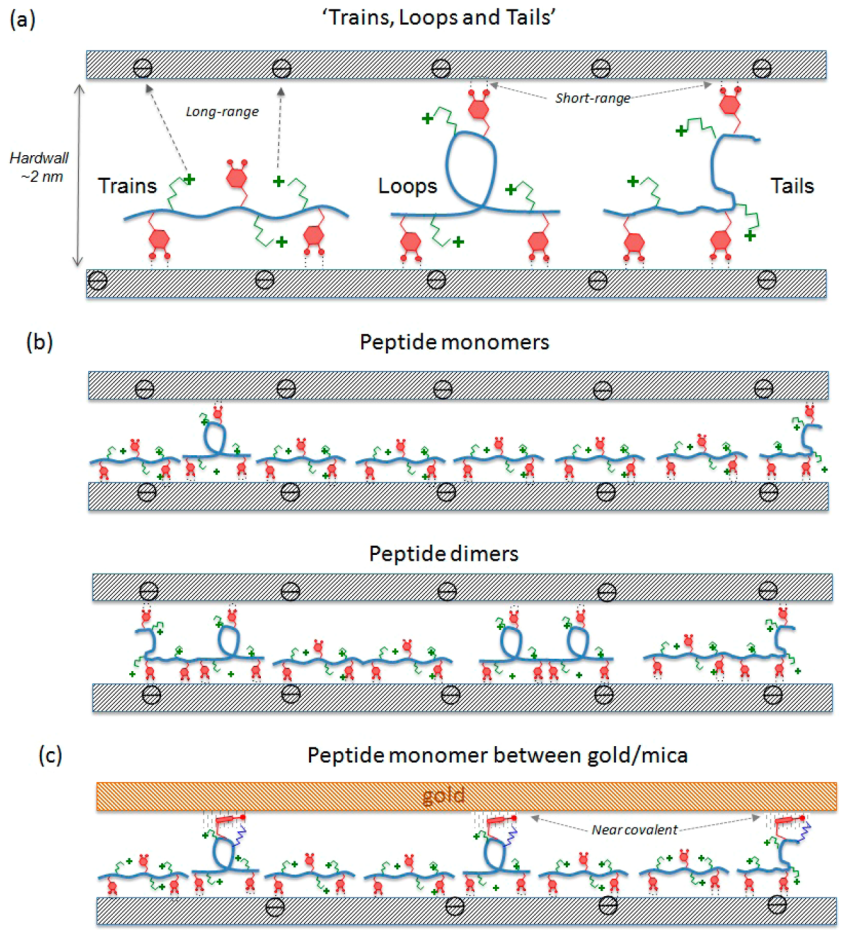

Figure 8. Binding models of peptides. (a) Different conformations of peptides on surface: train loop and tail. (b) Peptide monomers and dimers bridging two mica surfaces. (c) Peptide monomers bridging between mica and gold. The red side chains represent Dopa, green side chains represent positive charge (Lys), and blue ones represent side chains of the other amino acids.

interactions have angstrom length scales and require complementary target geometry for H-bond or coordination bond formation. As most biological molecules and surfaces are charged, long-range electrostatic interactions may serve to guide mussel adhesive proteins and various mussel inspired adhesive polymers toward target binding sites on substrate surfaces, paving the way for Dopa residues to make strong, specific bonds.[29,30]

Another major finding of this study is that increasing peptide length enhances Dopa-mediated bridging adhesion on surfaces. With Dopa residues scattered along the sequence, adhesive proteins or peptides have to be long enough to adopt appropriate conformations on one mica surface that enable the presentation of Dopa containing side chains to the other surface. All three mfp-5-derived short peptides showed adhesion energies that are at least an order of magnitude lower than the adhesion energy of intact mfp-5, about 7.1 mJ/m^2 (adjusted according to the Derjaguin approximation $F/2\pi R$), measured by the SFA.[5] Mfp-5 consists of about 74 amino acid residues, 20 of which are Dopa (~30 mol %). Given their size and flexible extended conformations, mfp-5 molecules are likely to have wormlike structures on the mica surface. The longer protein backbone and many Dopa side chains give mfp-5 molecules an excellent opportunity to bridge two surfaces and to have Dopa residues from the same backbone firmly planted on both sides (Figure 8).

The peptides, in contrast, are much shorter, with between 3 and 5 Dopa groups in their sequence. During the deposition, an entire peptide may stick as a train to one mica surface, leaving few or no "loops" or "tails" with Dopa groups to bridge to the other mica surface. This would result in fewer bridging opportunities (Figure 8). A critical peptide length in adhesion is supported by the SFA results of PEP-pI-4-dimer, which demonstrates that doubling the length of the peptide sequence roughly doubles the adhesive forces. This mechanism is consistent with polymer scaling theory, where, in the simplest picture, the mean-squared radius of a solvated polymer in solution, $\langle r^2\rangle^{1/2}$, scales as $N^{3/5}$, where N is the number of monomers along a polymer backbone. Thus, doubling the length of a 15−17 residue peptide should be expected to increase $\langle r^2\rangle^{1/2}$ by a factor of ~1.5, and increasing the length of a 15 residue peptide by a factor of 5 (mfp-5 is a 75-residue protein) should be expected to roughly increase $\langle r^2\rangle^{1/2}$ by a factor of ~2.63. Both cases demonstrate that increasingly compact and "looped" solution configurations of the proteins and peptides become highly favored with increasing length. DLS (Figure S5) shows pep-pI-4 monomer and dimer have similar hydrodynamic diameter in solution, which indicates dimer has more compact configuration than monomer. Since solution configurations are intimately connected to adsorption configurations in cases where polymers quickly and irreversibly bind to surfaces, we believe that on surfaces the dimer adopts a more compact configuration, too, which results in more "loops" and "tails" structure to stick to the second surface. When a peptide is deposited onto a surface, entropy maximization will be in competition with the chemical free energy reduction change by

DOI: 10.1021/la504316q
Langmuir 2015, 31, 1105−1112

Dopa/surface binding. With longer peptides, the entropic contribution to the free energy offered by adopting a random structure will win out over the free energy decrease due to chemical binding, which would result in peptides lying flat on surfaces. When the opposing surface is presented, a flexible random structure is more favorable for the peptide to bridge two surfaces when adhesion depends on forming Dopa mediated interactions on both sides.

The unevenly distributed Dopa binding of PEP-pI-10 is further suggested by the strong bridging adhesion (~3 mJ/m^2) of PEP-pI-10 in a gold/peptide/mica geometry by measuring the adhesion of a PEP-pI-10 deposited mica surface against an opposing gold surface in pH 3 buffer (Figure 7). On the peptide/gold interface, PEP-pI-10 interacts with the gold surface through "soft epitaxial" binding;[24] adding Dopa functions as a "surface anchor".[25] Thus, strong adhesion can be promoted between the mica and gold surfaces, even if few Dopa residues are available to interact with the gold surface. Further, assuming that the binding of PEP-pI-10 to mica is the weakest link in the peptide mediated bridge between gold and mica, the adhesion of 3 mJ/m^2 is about 40% of the value of intact mfp-5 on the mica surface.

Mussel adhesive proteins have inspired numerous investigations of Dopa- or catechol-functionalized synthetic materials for various applications including wet adhesives,[10,12,31−33] antifoulant coatings,[34,35] magnetic imaging agents,[36] tissue glues, and pH-sensitive hydrogels. Most of these materials have been designed by a trial-and-error approach after many costly and time-consuming iterations. We maintain that a systematic understanding of factors that contribute to bridging or coating adhesion in mussels proteins can accelerate the practical implementation of important design concepts.

CONCLUSION

The design and synthesis of mussel-inspired peptides allowed us to investigate the role of electrostatic—especially cationic—contributions to the bridging adhesion of Dopa-containing peptides. Electrostatic effects in the adhesion of mfp-5 were not previously detected, perhaps because of steric constraints imposed by the long native protein backbone. The chain-length-dependent adhesion of PEP-pI-4-dimers and monomers explicitly illustrates the significance of peptide length on promoting adhesion between two surfaces when the adhesion of peptides to each of the surfaces is dominated by Dopa-mediated interactions. Increasing chain length promotes increasingly disordered structures, rather than the flattened conformations where most, if not all, the Dopa-containing side chains are bound to a single surface, and thus promotes interaction with a second approaching surface. In this light, the strong adhesion of mfp-5 might result not only from its long sequence but also to synergistic or cooperative effects between amino acid residues over the whole protein sequence. Given the fact that nature has optimized mussel proteins for adhesion over millions of years, these synergistic effects should not be so surprising. Another important message conveyed by this study is that, in practice, when the second surface (e.g., gold) does not rely exclusively on Dopa for bridging adhesion, relatively short molecules can mediate bridging between different surfaces via different binding mechanisms even though Dopa residues have been mostly occupied by the first surface (e.g., mica). Analysis of adhesion by short mfp-derived peptide sequences provides a simpler way to design better mussel inspired adhesives for complex/heterogeneous surface chemistries and is more cost-effective from the engineering perspective.

EXPERIMENTAL SECTION

Peptide modification and purification: The peptides HYHSGGSYHGSGYHG (PEP-pI-6.5), VGSGYDGYSDGYYDG (PEP-pI-4), GYKGKYYGKGKKYYYK (PEP-pI-10), and VGSGYDGYSDGYYDGVGSGYDGYSDGYYDG (PEP-pI-4-dimer) were synthesized by GenScript (Piscataway, NJ) using routine solid-phase synthesis that included N-terminal acetylation and C-terminal amidation and were provided as a desalted solid. Mushroom tyrosinase (3000 U/mg) was from Aldrich-Sigma, and all other reagents were of analytical grade. *Enzymatic modification*: The peptides (1 mg) were dissolved in 1 mL of pH 7.0, 20 mM borate, 0.1 M phosphate-ascorbate buffer, in an Eppendorf microfuge tube. After adding mushroom tyrosinase (0.3 mg), the tube was shaken for 4 h at ambient room temperature and pressure. Each reaction was stopped by adding 40 μL of glacial acetic acid, and the resulting product was subjected to reverse phase HPLC column, eluted with a linear gradient of aqueous acetonitrile. Eluant was monitored continuously at 230 and 280 nm, and 0.33 mL fractions containing peptides were pooled and freeze-dried. Sample purity and hydroxylation were assessed by amino acid analysis and electrospray ionization mass spectrometry. Fractions with pure hydroxylated peptides were dissolved in 0.1 M acetic acid (Sigma-Aldrich) and 0.25 M potassium nitrate (Sigma-Aldrich) buffer (pH 3) with a peptide concentration of 100 μg/mL and kept in a −80 °C freezer.

Mass spectroscopy: A Micromass QTOF2 tandem mass spectrometer (Waters Corp.) with an electrospray ionization source and matrix assisted laser desorption ionization (MALDI) with time-of-flight mass (TOF) (Bruker Microflex LRF) were used to obtain spectrometry of peptides. For QTOF2-ESI, samples were infused at 10 μL/min via a Harvard Apparatus syringe pump. Capillary voltage was held at 3.5 kV. Source and desolvation temperatures were 80 and 100 °C, respectively. MS/MS experiments were carried out with argon as collision gas and a collision voltage of 10 V. For MALDI-TOF, the N_2 laser (337 nm) fires at 60 Hz. 1−2 μL of sample peptide was spotted onto the gold-plated sample plate and vacuum-dried, on top of which 1 μL of matrix solution (α-cyano-3-hydroxycinnamic acid in aqueous 50% acetonitrile and 0.1% trifluoroacetic acid) was added. External calibrant was peptide calibration standard mixture from Bruker containing seven standard peptides with a mass range between ~1000 and 3500 Da.

Amino acid analysis: The amino acid composition of the hydrolyzed peptides was determined on a Hitachi L8900 amino acid analyzer system with ninhydrin detection. Polypeptides were hydrolyzed in 100 μL of 6 M HCl with 8% phenol in vacuum at 158 °C for 40 min. After being washed with water and methanol, the hydrolyzed products were dissolved in 0.2 M HCl and injected into amino acid analyzer.

Surface forces apparatus (SFA): The adhesion of each peptide to mica was then measured by a SFA in a reported configuration. Prior to each experiment, 10 μL of peptide solution was added on top of 1 mica surface, letting the peptide adsorb on mica for 20 min followed by rinsing excessively with the same buffer to remove the nonadsorbed peptide molecules. The adhesion force measured was normalized by the radius of curved disks used in the SFA experiment, typically 2 cm, and further converted into adhesion energy (or work of adhesion) by using the Derjaguin approximation: $E = F/2\pi R$.

Dynamic light scattering: The sizes of pep-pI-4 monomer and dimer in solution (2 mg/mL) in 100 mM acetic acid and 100 mM acetic acid containing 0.25 M KNO_3 were obtained using the Malvern Nano ZS, which is calibrated regularly using Malvern Zeta Potential Transfer standard (P/N DTS1230, batch number 380901).

ASSOCIATED CONTENT

Supporting Information

Figures S1−S5. This material is available free of charge via the Internet at http://pubs.acs.org.

AUTHOR INFORMATION

Corresponding Author

*E-mail herbert.waite@lifesci.ucsb.edu (J.H.W.).

DOI: 10.1021/la504316q
Langmuir 2015, 31, 1105−1112

Author Contributions

W.W., J.Y., and M.A.G. contributed equally to this work.

Notes

The authors declare no competing financial interest.

■ ACKNOWLEDGMENTS

This work was supported by the Materials Research Science and Engineering Centers Program of the National Science Foundation under Award DMR 1121053 and the National Institutes of Health under Grant R01-DE018468.

■ REFERENCES

(1) Stewart, R. J.; Weaver, J. C.; Morse, D. E.; Waite, J. H. The tube cement of Phragmatopoma californica: a solid foam. *J. Exp. Biol.* **2004**, *207*, 4727−4734.

(2) Lee, B. P.; Messersmith, P. B.; Israelachvili, J. N.; Waite, J. H. Mussel-inspired adhesives and coatings. *Annu. Rev. Mater. Res.* **2011**, *41*, 99−132.

(3) Anderson, T. H.; Yu, J.; Estrada, A.; Hammer, M. U.; Waite, J. H.; Israelachvili, J. N. The contribution of DOPA to substrate-peptide adhesion and internal cohesion of mussel-inspired synthetic peptide films. *Adv. Funct. Mater.* **2010**, *20*, 4196−4205.

(4) Lee, H.; Scherer, N. F.; Messersmith, P. B. Single-molecule mechanics of mussel adhesion. *Proc. Natl. Acad. Sci. U. S. A.* **2006**, *103*, 12999−13003.

(5) Danner, E. W.; Kan, Y.; Hammer, M. U.; Israelachvili, J. N.; Waite, J. H. Adhesion of mussel foot protein Mefp-5 to mica: An underwater superglue. *Biochemistry* **2012**, *51*, 6511−6518.

(6) Lin, Q.; Gourdon, D.; Sun, C. J.; Holten-Andersen, N.; Anderson, T. H.; Waite, J. H.; Israelachvili, J. N. Adhesion mechanisms of the mussel foot proteins mfp-1 and mfp-3. *Proc. Natl. Acad. Sci. U. S. A.* **2007**, *104*, 3782−3786.

(7) Lu, Q.; Hwang, D. S.; Liu, Y.; Zeng, H. Molecular interactions of mussel protective coating protein, mcfp-1, from Mytilus californianus. *Biomaterials* **2012**, *33*, 1903−1911.

(8) Qin, Z.; Buehler, M. Molecular mechanics of dihydroxyphenylalanine at a silica interface. *Appl. Phys. Lett.* **2012**, *101*, 083702−4.

(9) Yu, J.; Wei, W.; Danner, E.; Ashley, R. K.; Israelachvili, J. N.; Waite, J. H. Mussel protein adhesion depends on interprotein thiol-mediated redox modulation. *Nat. Chem. Biol.* **2011**, *7*, 588−590.

(10) Wang, J. J.; Tahir, M. N.; Kappl, M.; Tremel, W.; Metz, N.; Barz, M.; Theato, P.; Butt, H. J. Influence of binding-site density in wet bioadhesion. *Adv. Mater.* **2008**, *20*, 3872.

(11) Matos-Perez, C. R.; White, J. D.; Wilker, J. J. Polymer composition and substrate influences on the adhesive bonding of a biomimetic, cross-linking polymer. *J. Am. Chem. Soc.* **2012**, *134*, 9498−9505.

(12) You, I.; Kang, S. M.; Lee, S.; Cho, Y. O.; Kim, J. B.; Lee, S. B.; Nam, Y. S.; Lee, H. Polydopamine microfluidic system toward a two-dimensional, gravity-driven mixing device. *Angew. Chem., Int. Ed.* **2012**, *51*, 6126−6130.

(13) Mann, L. K.; Papanna, R.; Moise, K. J.; Byrd, R. H.; Popek, E. J.; Kaur, S.; Tseng, S. C. G.; Stewart, R. J. Fetal membrane patch and biomimetic adhesive coacervates as a sealant for fetoscopic defects. *Acta Biomater.* **2012**, *8*, 2160−2165.

(14) Brubaker, C. E.; Messersmith, P. B. Enzymatically degradable mussel-inspired adhesive hydrogel. *Biomacromolecules* **2011**, *12*, 4326−4334.

(15) Krivosheeva, O.; Dedinaite, A.; Claesson, P. M. Adsorption of Mefp-1: Influence of pH on adsorption kinetics and adsorbed amount. *J. Colloid Interface Sci.* **2012**, *379*, 107−113.

(16) Israelachvili, J.; Min, Y.; Akbulut, M.; Alig, A.; Carver, G.; Greene, W.; Kristiansen, K.; Meyer, E.; Pesika, N.; Rosenberg, K.; Zeng, H.: Recent advances in the surface forces apparatus (SFA) technique. *Rep. Prog. Phys.* **2010**, *73*.

(17) Taylor, S. W. Chemoenzymatic synthesis of peptidyl 3,4-dihydroxyphenylalanine for structure-activity relationships in marine invertebrate polypeptides. *Anal. Biochem.* **2002**, *302*, 70−74.

(18) Wilke, P.; Borner, H. G. Mussel-glue derived peptide-polymer conjugates to realize enzyme-activated antifouling coatings. *ACS Macro Lett.* **2012**, *1*, 871−875.

(19) Patwardhan, S. V. E.; F, S.; Berry, R. J.; Jones, S. E.; Naik, R. R.; Deschaume, O.; Heinz, H.; Perry, C. C. Chemistry of aqueous silica nanoparticle surfaces and the mechanism of selective peptide adsorption. *J. Am. Chem. Soc.* **2012**, *134*, 6244−6256.

(20) Israelachvili, J. N. *Intermolecular and Surface Forces*, 3rd ed.; Academic Press: Burlington, MA, 2011.

(21) Hartvig, R. A.; van de Weert, M.; Ostergaard, J.; Jorgensen, L.; Jensen, H. Protein adsorption at charged surfaces: The role of electrostatic interactions and interfacial charge regulation. *Langmuir* **2011**, *27*, 2634−2643.

(22) Khandelia, H.; Kaznessis, Y. N. Cation-pi interactions stabilize the structure of the antimicrobial peptide indolicidin near membranes: Molecular dynamics simulations. *J. Phys. Chem. B* **2007**, *111*, 242−250.

(23) Shi, Z. S.; Olson, C. A.; Kallenbach, N. R. Cation-pi interaction in model alpha-helical peptides. *J. Am. Chem. Soc.* **2002**, *124*, 3284−3291.

(24) Feng, J. P., R B.; Berry, R. J.; Farmer, B. L.; Naikc, R. R.; Heinz, H.: Adsorption mechanism of single amino acid and surfactant molecules to Au {111} surfaces in aqueous solution: design rules for metal-binding molecules. *Soft Matter* **2010**, *7*.

(25) Weinhold, M.; Soubatch, S.; Temirov, R.; Rohlfing, M.; Jastorff, B.; Tautz, F. S.; Doose, C. Structure and bonding of the multifunctional amino acid L-DOPA on Au(110). *J. Phys. Chem. B* **2006**, *110*, 23756−23769.

(26) Plekan, O.; Feyer, V.; Ptasinska, S.; Tsud, N.; Prince, K. C. Cyclic dipeptide immobilization on Au(111) and Cu(110) surfaces. *Phys. Chem. Chem. Phys.* **2014**, *16*, 6657−6665.

(27) Humblot, V.; Tejeda, A.; Landoulsi, J.; Vallée, A.; Naitabdi, A.; Taleb, A.; Pradier, C. M. Walking peptide on Au(110) surface: Origin and nature of interfacial process. *Surf. Sci.* **2014**, *628*, 21−29.

(28) Heinz, H.; Farmer, B. L.; Pandey, R. B.; Slocik, J. M.; Patnaik, S. S.; Pachter, R.; Naik, R. R. Nature of molecular interactions of peptides with gold, palladium, and Pd-Au bimetal surfaces in aqueous solution. *J. Am. Chem. Soc.* **2009**, *131*, 9704−9714.

(29) Valtiner, M.; Donaldson, S. H.; Gebbie, M. A.; Israelachvili, J. N. Hydrophobic forces, electrostatic steering, and acid-base bridging between atomically smooth self-assembled monolayers and end-functionalized PEGolated lipid bilayers. *J. Am. Chem. Soc.* **2012**, *134*, 1746−1753.

(30) Heinz, H. The role of chemistry and pH of solid surfaces for specific adsorption of biomolecules in solution—accurate computational models and experiment. *J. Phys.: Condens. Matter* **2014**, *26*, 244105.

(31) Lee, H.; Dellatore, S. M.; Miller, W. M.; Messersmith, P. B. Mussel-inspired surface chemistry for multifunctional coatings. *Science* **2007**, *318*, 426−430.

(32) Park, K. M.; Park, K. D. Facile surface immobilization of cell adhesive peptide onto TiO_2 substrate via tyrosinase-catalyzed oxidative reaction. *J. Mater. Chem.* **2011**, *21*, 15906−15908.

(33) Shafiq, Z.; Cui, J. X.; Pastor-Perez, L.; San Miguel, V.; Gropeanu, R. A.; Serrano, C.; del Campo, A. Bioinspired underwater bonding and debonding on demand. *Angew. Chem., Int. Ed.* **2012**, *51*, 4332−4335.

(34) Kuang, J. H.; Messersmith, P. B. Universal surface-initiated polymerization of antifouling zwitterionic brushes using a mussel-mimetic peptide initiator. *Langmuir* **2012**, *28*, 7258−7266.

(35) Dalsin, J. L.; Hu, B. H.; Lee, B. P.; Messersmith, P. B. Mussel adhesive protein mimetic polymers for the preparation of nonfouling surfaces. *J. Am. Chem. Soc.* **2003**, *125*, 4253−4258.

(36) Lee, Y. H.; Lee, H.; Kim, Y. B.; Kim, J. Y.; Hyeon, T.; Park, H.; Messersmith, P. B.; Park, T. G. Bioinspired surface immobilization of hyaluronic acid on monodisperse magnetite nanocrystals for targeted cancer imaging. *Adv. Mater.* **2008**, *20*, 4154.

DOI: 10.1021/la504316q
Langmuir 2015, 31, 1105−1112